A General Magnetic-Energy-Based Torque Estimator: Validation via a Permanent-Magnet Motor Drive

Calum Cossar, Mircea Popescu, *Senior Member, IEEE*, T. J. E. Miller, *Fellow, IEEE*, Malcolm McGilp, and Mircea Olaru

***Abstract*—This paper describes the use of the current–flux-linkage ($i-\psi$) diagram to validate the performance of a general magnetic-energy-based torque estimator. An early step in the torque estimation is the use of controller duty cycles to reconstruct the average phase-voltage waveform during each pulsewidth-modulation (PWM) switching period. Samples over the fundamental period are recorded for the estimation of the average torque. The fundamental period may not be an exact multiple of the sample time. For low speed, the reconstructed voltage requires additional compensation for inverter-device losses. Experimental validation of this reconstructed waveform with the actual PWM phase-voltage waveform is impossible due to the fact that one is PWM in nature and the other is the average value during the PWM period. A solution to this is to determine the phase flux-linkage using each waveform and then plot the resultant $i-\psi$ loops. The torque estimation is based on instantaneous measurements and can therefore be applied to any electrical machine. This paper includes test results for a three-phase interior permanent-magnet brushless ac motor operating with both sinusoidal and nonsinusoidal current waveforms.**

***Index Terms*—Brushless permanent-magnet (PM) motor drives, electromagnetic average torque, torque estimator.**

I. Introduction

In THE last decade, brushless permanent-magnet (PM) motor drives have been widely used in many industrial applications such as robots, rolling mills, or machine tools. The advantages of these machines include high power density, low inertia, and high-speed capabilities. However, the control performance of the PM motors is greatly affected by the uncertainties related to the motor parameters, external load disturbance, and unmodeled and nonlinear dynamics [3]. Advanced control techniques such as nonlinear control [4], adaptive control [5], robust control [6], variable structure control, and intelligent control have been developed. However, the overall stability may not be guaranteed in these schemes due to certain assumptions introduced, complicated controller design, and feedback linearization.

This paper proposes a new torque estimator that can be used for online measurement of the average torque for any type of brushless PM motor drive. From the phase-current and phase-voltage measurements, the flux-linkage values are estimated. With phase currents and flux linkages available, the average torque is estimated online with high accuracy. The proposed estimator avoids the classical dq transformation [4], [6] and, thus, is applicable to any PM motor drive, regardless of the control strategy, winding distribution, saturation level, and/or number of slots/pole. This robust scheme may be implemented in a digital signal processor (DSP) and used not only for measurement of the average torque without any torque transducers but it may be successfully implemented in any torque controller that requires the average torque estimation. The proposed algorithm is validated experimentally and theoretically through the usage of the $i-\psi$ diagram.

II. Mathematical Model

The method of energy functional variation, which uses a derivative of the magnetic energy with respect to position at constant flux linkages or the derivative of magnetic coenergy with respect to position at constant current to compute the electromagnetic torque, is generally accepted as a method well suited for torque estimation [1], [2].

The instantaneous electromagnetic torque may be found as a derivative of the magnetic energy with respect to position at constant flux linkages or the derivative of magnetic coenergy with respect to position at constant current

$$T_{\mathrm{e}} = -\left.\frac{\partial W}{\partial \theta}\right|_{\psi=\mathrm{ct}} = \left.\frac{\partial W'}{\partial \theta}\right|_{i=\mathrm{ct}}. \tag{1}$$

The total magnetic-field energy produced by a system of n coils having the flux linkages $\psi_1, \psi_2, \ldots, \psi_n$ and the currents $i_1, i_2, \ldots, i_n$ is given by

$$W + W' = \sum_{k=1}^{n} i_k \psi_k. \tag{2}$$

In a conservative (lossless) system, this energy equals the sum of the magnetostatic energy of the system (i.e., motor) and the

Paper IPCSD-MT08-02, presented at the 2006 Industry Applications Society Annual Meeting, Tampa, FL, October 8–12, and approved for publication in the IEEE TRANSACTIONS ON INDUSTRY APPLICATIONS by the Industrial Drives Committee of the IEEE Industry Applications Society. Manuscript submitted for review November 4, 2006 and released for publication December 6, 2007. Published July 23, 2008 (projected).

C. Cossar, M. Popescu, T. J. E. Miller, and M. McGilp are with the SPEED Laboratory, Department of Electronics and Electrical Engineering, University of Glasgow, Glasgow, G12 8LT, U.K. (e-mail: calum@elec.gla.ac.uk; mircea@elec.gla.ac.uk; t.miller@elec.gla.ac.uk; mal@elec.gla.ac.uk).

M. Olaru is with ICNDMF-CEFIN, 70314 Bucharest, Romania (e-mail: mirceaolaru2@yahoo.com).

Color versions of one or more of the figures in this paper are available online at http://ieeexplore.ieee.org.

Digital Object Identifier 10.1109/TIA.2008.926231

mechanical work

$$\Delta(W+W') = \left(\sum_{k=1}^{n} i_k \Delta\psi_k + \sum_{k=1}^{n} \psi_k \Delta i_k\right) = \Delta W_m + T_e \Delta\theta. \quad (3)$$

From (1)–(3), if we neglect the stored magnetostatic energy, we obtain

$$T_{\rm e} = \frac{1}{2} \cdot \frac{\sum_{k=1}^{n} i_k \Delta\psi_k \Big|_{i=\rm ct}}{\Delta\theta} - \frac{1}{2} \cdot \frac{\sum_{k=1}^{n} \psi_k \Delta i_k \Big|_{\psi=\rm ct}}{\Delta\theta}. \quad (4)$$

By integrating over a fundamental cycle, we can obtain the average electromagnetic torque

$$T_{\rm avg} = \frac{1}{2T\Delta\theta} \cdot \int_0^T \left(\sum_{k=1}^{n} i_k \Delta\psi_k - \sum_{k=1}^{n} \psi_k \Delta i_k\right) dt. \quad (5)$$

If we use the relation

$$\psi_k = \int_0^T (v_k - r_k i_k) dt \quad (6)$$

and dividing a fundamental cycle in N samples, expression (5) becomes

$$T_{\rm avg} = \frac{p}{2\pi} \cdot \sum_{i=1}^{N} \left[\sum_{k=1}^{n} i_k \Delta \sum_{j=1}^{n} (v_j - r_k i_j)_k - \sum_{k=1}^{n} \Delta i_k \sum_{j=1}^{n} (v_j - r_k i_j)_k\right]. \quad (7)$$

Relation (7) suggests that, if the phase currents and voltages are measured online, a general torque estimator may be implemented for any motor type. When demonstrating (7), no assumption was made to restrict this approach to a certain motor type or to a linear system. This paper is dedicated to the implementation and validation of a new torque estimator based on (7) to the PM motor drives. The average electromagnetic torque is equivalent to the torque predicted by the $i-\psi$ diagram [1] or the flux–MMF diagram [2] and is proportional to the area enclosed by the $i-\psi$ locus over one fundamental cycle

$$T_{\rm avg} = \frac{mp}{2\pi} \Delta W' \quad (8)$$

where $\Delta W'$ is the coenergy or energy converted per phase during the fundamental period, m is the number of phases, and p is the number of pole pairs.

III. Average Torque Estimator

The proposed average torque estimation is based around the relationship between coenergy and average torque. As we have seen, the coenergy is proportional to the area enclosed by the $i-\psi$ locus over one fundamental cycle, but it can also be calculated from measuring the energy supplied to the phase over one fundamental cycle and subtracting the energy loss associated with the phase resistance. Given a digital implementation using high-frequency sampling, the total energy supplied to the phase during a fundamental cycle is

$$(W)_{\rm cycle} = \left(\sum_{0}^{N} i_{\rm ph} v_{\rm ph}\right) \tau_{\rm cycle} \quad (9)$$

where N is the number of samples in one fundamental cycle and $\tau_{\rm cycle}$ is the fundamental period.

The resistive energy loss over one complete cycle is given by

$$W_{\rm Cu} = (I_{\rm rms})^2 R_{\rm ph} \tau_{\rm cycle}. \quad (10)$$

$(I_{\rm rms})^2$ is equivalent to the mean-squared current and, in a sampling system, can be calculated for any current waveform as follows:

$$(I_{\rm rms})^2 = \frac{1}{N}\left[\sum_{0}^{N} (i_{\rm ph})^2\right]. \quad (11)$$

Hence, corresponding to the fundamental cycle, the phase-energy/coenergy variation can be calculated using the following expression and then substituted in (8):

$$\Delta W' = \left(\sum_{0}^{N} i_{\rm ph} v_{\rm ph}\right) \tau_{\rm cycle} - \frac{1}{N}\left(\sum_{0}^{N} (i_{\rm ph})^2\right) R_{\rm ph} \tau_{\rm cycle}. \quad (12)$$

In measurement terms, the torque estimator is therefore required to sample the phase current and phase voltage every switching period over a complete fundamental cycle and also determine the time taken for the fundamental cycle and the related number of samples during this time. It is worthwhile considering the effects on precision when the fundamental period is not an integral number of samples. For a 50-μs sample period, there are 1200 samples for a motor speed of 1000 r/min; similarly for 3600 r/min, there are 333 samples; therefore, the effect becomes more significant as the speed increases. If high-speed operation is required, then the solution would be to decrease the sample period; for the test platform described in the next section, a sample period of 10 μs is achievable.

The torque estimator is implemented on a general-purpose motor control platform which may be used to implement a range of control strategies for brushless PM and switched-reluctance machines. The controller is based on a low-cost TI C280 150-MHz 32-bits fixed-point DSP; a summary of its applicable hardware peripherals being as follows: synchronized six-phase 12-bits pulsewidth-modulation (PWM) outputs at 20 kHz; dedicated incremental encoder interface; 16–12-bits analog-to-digital converter channels; and asynchronous and synchronous communication ports. The controller hardware also includes a four-channel 12-bits digital-to-analog converter to allow analog representations of controller parameters such as sampled phase currents to be output to an oscilloscope. This becomes very useful in facilitating the validation of the

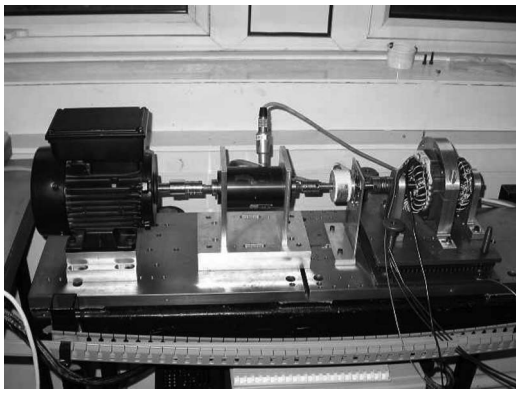

Fig. 1. Experimental test stand.

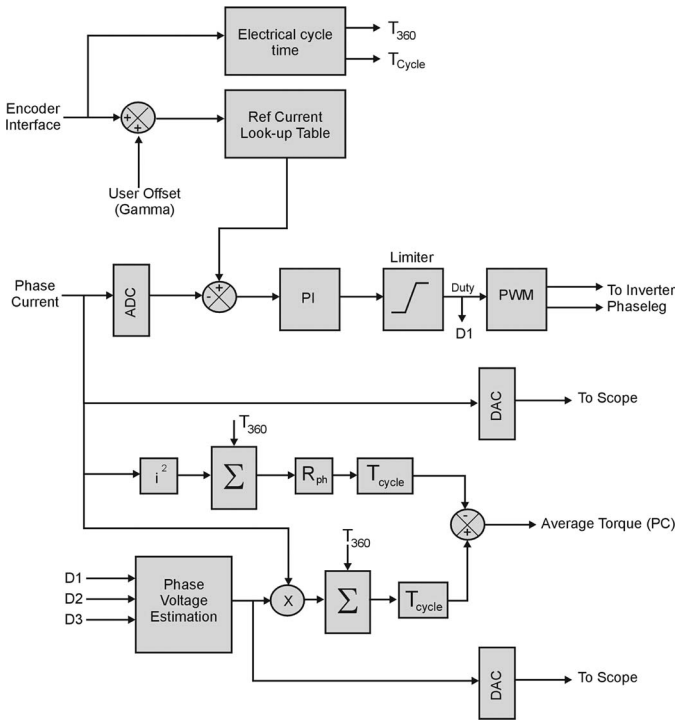

Fig. 2. Controller and torque estimator for a PMAC motor.

torque estimator as described later. The motor-control strategies and associated torque estimator are all implemented in DSP software with an inner current/torque control loop running at 20 kHz. Note that, as the torque estimator is using instantaneous measurements and the subsequent calculations are based on stored-energy conservation, the technique can be applied to any electrical machine—for example, brushless PM, induction, and switched-reluctance motors. The bandwidth response of this torque estimator limits its application to the case of drive systems where it is required to find an optimized high-efficiency steady-state operating point.

IV. Experimental Tests and Validation

Experimental tests are carried out on a three-phase wye-connected PM ac motor running with both sinusoidal and nonsinusoidal phase currents. A photograph of the experimental test rig is shown in Fig. 1. The laboratory test machine is a

TABLE I
THREE-PHASE INVERTER SWITCHING STATES

Switch States	Phase Connections	Resultant Phase 1 Voltage
Phase 1 = U Phase 2 = U Phase 3 = U	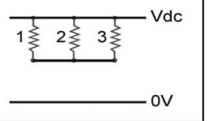	$v_{ph} = 0$
Phase 1 = L Phase 2 = L Phase 3 = L	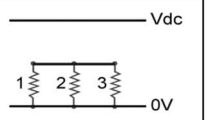	$v_{ph} = 0$
Phase 1 = U Phase 2 = L Phase 3 = L	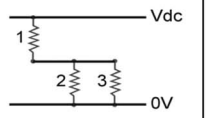	$v_{ph} = +\frac{2}{3}V_{DC}$
Phase 1 = U Phase 2 = U Phase 3 = L	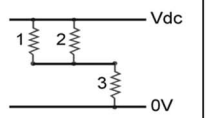	$v_{ph} = +\frac{1}{3}V_{DC}$
Phase 1 = L Phase 2 = U Phase 3 = U	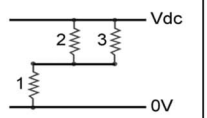	$v_{ph} = -\frac{2}{3}V_{DC}$
Phase 1 = L Phase 2 = L Phase 3 = U	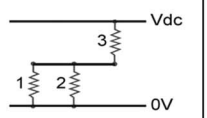	$v_{ph} = -\frac{1}{3}V_{DC}$
Phase 1 = L Phase 2 = U Phase 3 = L	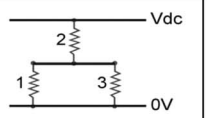	$v_{ph} = -\frac{1}{3}V_{DC}$
Phase 1 = U Phase 2 = L Phase 3 = U	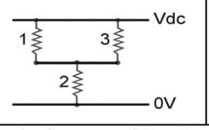	$v_{ph} = +\frac{1}{3}V_{DC}$

(Note: U = Upper phaseleg device on and L = Lower phaseleg device on.)

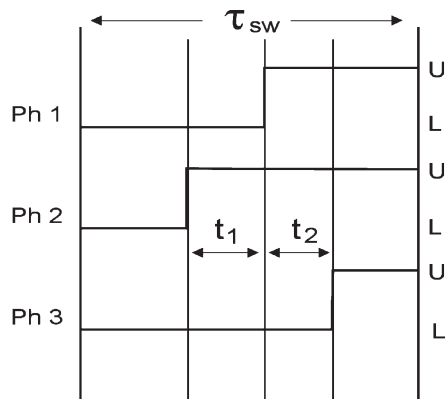

Fig. 3. Example of the PWM switching pattern.

fractional horsepower two-pole machine developed for use in an electrical appliance.

An outline of the interior PM (IPM) ac-motor control strategy (for one phase only) and the associated torque estimator is shown in Fig. 2. The basic requirement of the controller is

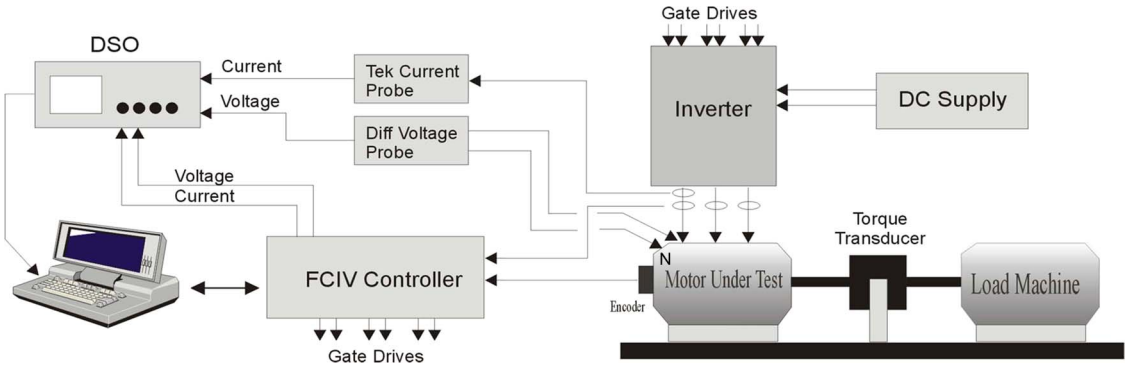

Fig. 4. Torque-estimation validation test rig.

to regulate each of the three phase currents such that they follow the associated sinusoidal-current references, which are synchronized with the rotor-back electromotive forces (EMFs), by the incremental encoder interface.

We have the following points to note. 1) This is just one of a number of possible current-control strategies; the proposed torque estimator is independent of this and will work with any PWM control strategy. 2) The torque estimator will function when additional outer speed and position control loops are included. For the calculation of the average torque, the controller must measure the following operating parameters over one fundamental cycle: the sampled phase current, the sampled phase voltage, and the number of samples in the fundamental cycle. The sampling period is fixed at 50 μs, and so, the number of samples varies as a function of speed.

For a three-phase wye-connected winding, the phase currents can be measured directly from the output current transducers in the controller/inverter. Phase voltage is not generally measured by the motor controller, and sometimes, it is not even possible to measure if the wye point is not available at the motor terminals, and so, this has to be derived from the duty-cycle values at every sample/switching period. The calculation method for the phase voltage is detailed in Table I, which outlines all the possible switch states and the resultant phase-one voltage if this state is valid throughout the high-frequency switching period. Note that, for a clear description of the method, all inverter voltage drops are omitted at this point. The derivation of the equivalent phase voltage is outlined in the example switching pattern shown in Fig. 3. Using Table I as reference, the average voltage during this switching period is

$$v_{\rm ph} = \frac{V_{\rm DC}}{3\tau_{\rm sw}}(t_2 - t_1). \tag{13}$$

Given the reconstructed nature of this phase-voltage waveform and the fact that various practical implementation effects such as inverter-device voltage drops and dead time had been neglected, it was considered important to attempt to validate this calculation with measured data. Direct comparison of an analog representation of this waveform with the output of a differential-voltage probe connected across phase one and the motor wye point was of little use, as the actual phase voltage included the high-frequency PWM component, and the estimated voltage consisted of samples representing the average

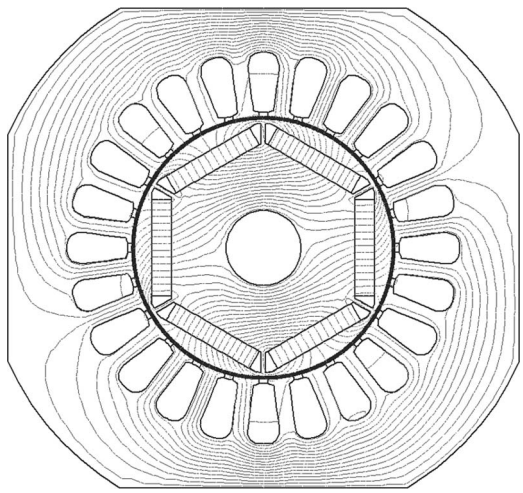

Fig. 5. Cross section with flux lines under load for the tested motor.

phase voltage over the switching period. One solution to this is to calculate phase flux linkage over an entire fundamental cycle and, then, plot the resultant $i-\psi$ loops for each case.

The flux linkage can be calculated using (5). The integration of the voltage is the key in allowing the comparison of the different voltage representations. The experimental validation-test setup is shown in Fig. 4. One fundamental cycle of measured current and voltage waveforms and the analog outputs of current and voltage from the controller is sampled by the digital storage oscilloscope. These data are then transferred to a PC, which performs the necessary calculation of flux linkages and plots the resultant $i-\psi$ loops. A comparison between the loop energy obtained with (12) and the measured one from the flux linkage and current is given in the Appendix. Fig. 5 shows the cross section with flux plot of the tested motor: a two-pole brushless IPM motor. Each magnet pole comprises three separate NdFeB magnets. The three-phase winding is wye connected and approximately sinewave distributed. There is no skew. Note the noncircular shape of the stator lamination and the corresponding complex pattern of saturation. These are causing a minor imbalance between the phase flux linkages. A theoretical validation is carried out for both sinusoidal and nonsinusoidal current waveforms. Two illustrative example results are shown in Figs. 6 and 7, where the solid line is obtained using (5) from the measured variables, while the thin dotted line shows the loop computed using a finite-element program [7].

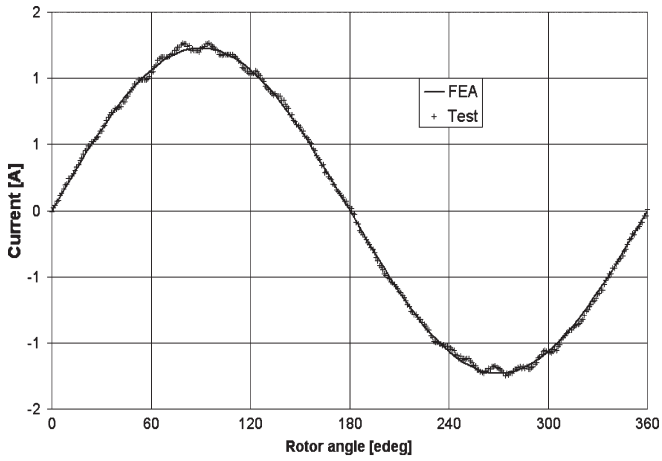

(a)

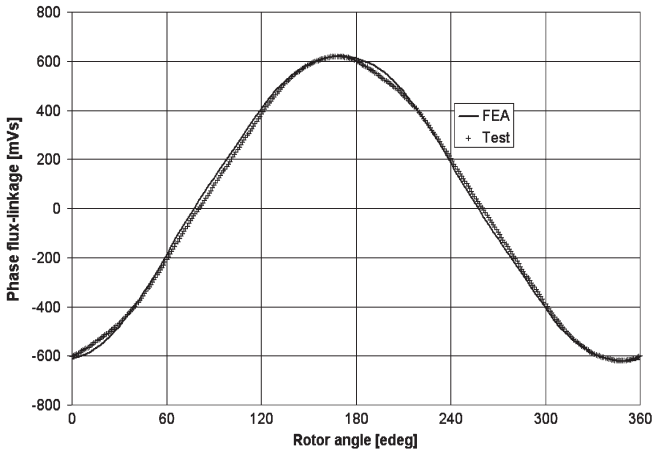

(b)

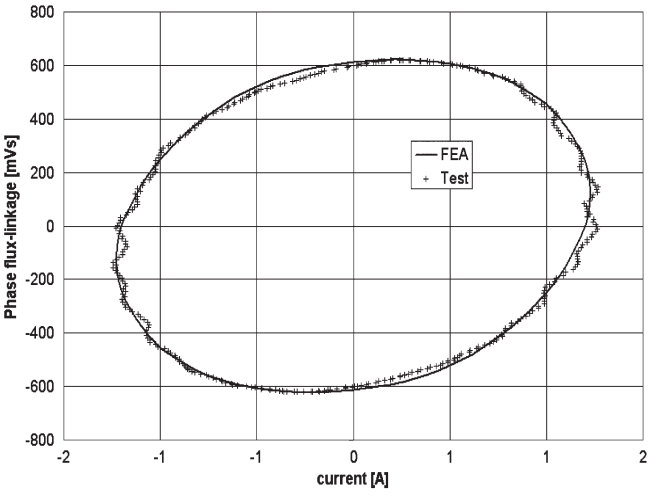

(c)

Fig. 6. (a) Sinusoidal current waveform. (b) Flux-linkage waveform for sinusoidal phase current. (c) $i-\psi$ loop for sinusoidal phase current.

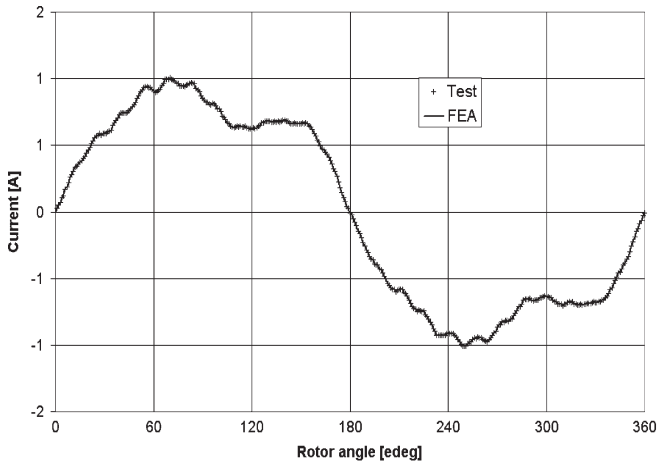

(a)

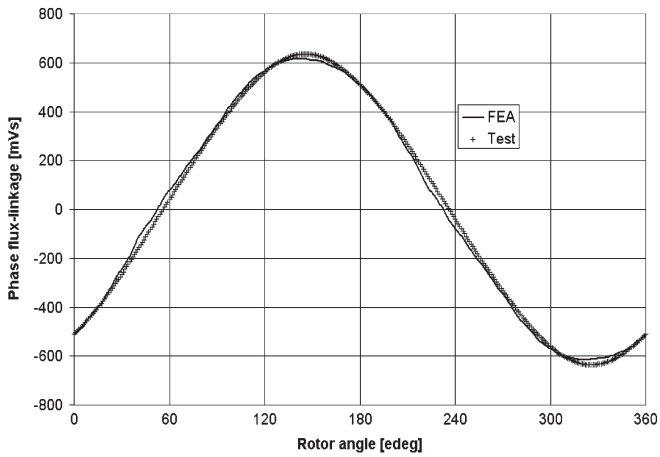

(b)

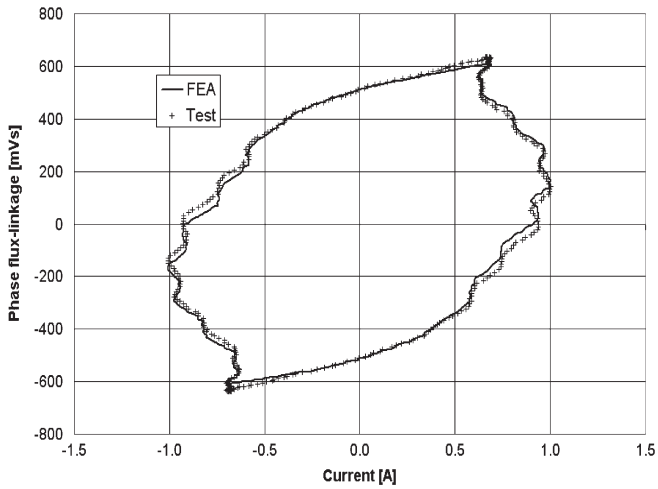

(c)

Fig. 7. (a) Nonsinusoidal current waveform. (b) Flux-linkage waveform for nonsinusoidal phase current. (c) $i-\psi$ loop for nonsinusoidal phase current.

There is a close correlation of the $i-\psi$ loops for both operating cases, both in terms of the resultant area of the loops and, more importantly, in terms of the shape of the loops. An experimental validation is carried out to compare online estimated torque with measured torque from a rotational torque transducer. Initial results are shown in Fig. 8(a), highlighting the increasing error in the online torque measurement as the speed is decreased.

A subsequent modification to the torque estimation to include a fixed voltage drop due to inverter-device losses during the "0 V" switching states improved performance considerably, as shown in Fig. 8(b). The "0 V" states are increasingly dominant at low speed due to the reduced-voltage requirements, so even although the device voltage drops are low, the time spent in

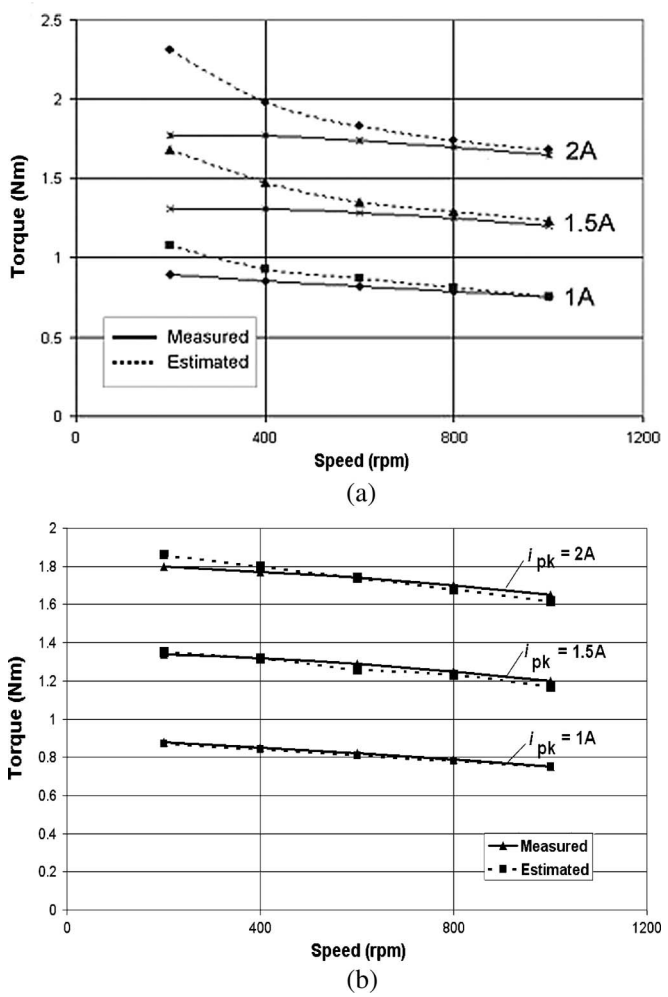

Fig. 8. Comparison of estimated versus measured torque values for sinusoidal phase currents with control angle (gamma) $= 0$. (a) No voltage compensation during "0 V" switching states. (b) Voltage compensation during "0 V" switching states.

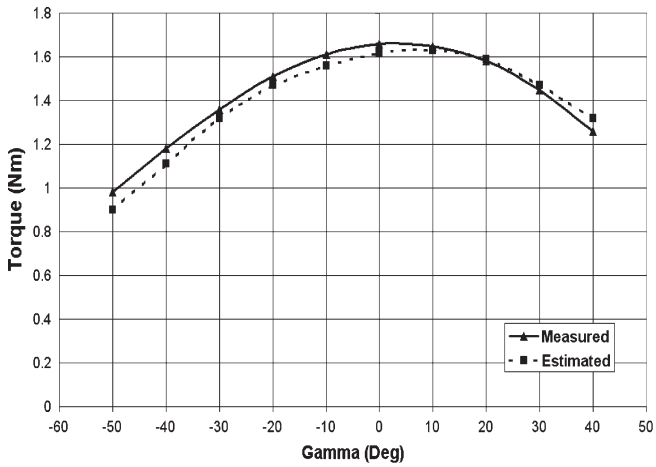

Fig. 9. Sinusoidal current case. Torque versus control angle (gamma) with speed $=$ 700 r/min and voltage compensation during "0 V" switching states.

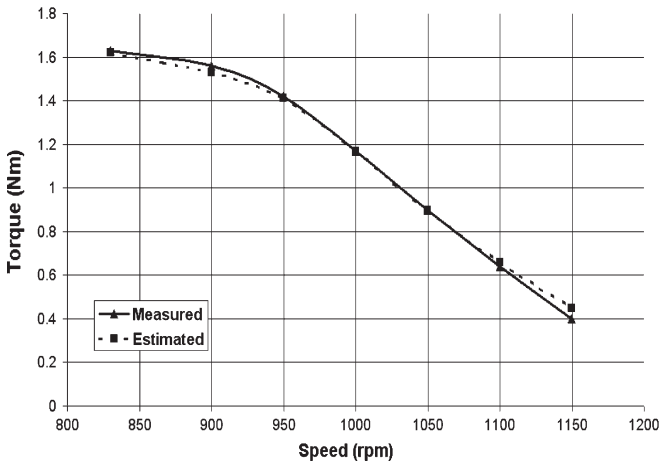

Fig. 10. Nonsinusoidal current case. Torque versus speed without voltage compensation during "0 V" switching states.

these states becomes significant, and compensation is increasingly required. Very low speed testing (< 100 r/min) was not possible with this machine due to dynamometer limitations, but it is expected that voltage compensation becomes even more critical in this speed range with the possible need for a more complex compensation strategy as compared to the presented fixed voltage drop set by the peak current.

This, however, would not be relevant in the main application of this technique; to optimize, online, the efficiency of variable-speed drives at any given operating point.

The possibility of extracting and displaying the information related to the $i-\psi$ loops from the data stored by the online torque estimator represents a very useful diagnosis tool. We get a measure of the torque ripple from the loop shape, and any unbalanced condition on the stator winding can be traced if the $i-\psi$ loops per phase are not identical in shape and area. As the estimated values through the online estimator algorithm described at Section III are practically identical with those obtained through the $i-\psi$ loop area (7), further results show just the comparison between the measured torque values (torque transducer) and the estimated torque values with the online estimator. Fig. 8 shows the torque variation with speed for three sinewave current levels, with amplitudes 1, 1.5, and 2 A and with current phasor aligned with the back EMF phasor, i.e., control angle (gamma) is zero. Note the difference due to the compensation voltage factor at low speed.

Fig. 9 shows the average torque variation for a sinusoidal current waveform with 2-A peak value, 700 r/min, and various control-angle (gamma) ranges.

For a complete analysis, the flux-weakening region results are shown in Fig. 10, when the current waveform is nonsinusoidal.

As motor speed increases, the required phase voltages to maintain sinusoidal phase currents also increases such that, at a given speed, the voltage demand exceeds that which is possible from the inverter/dc link; the result being increased distortion on the phase current waveforms, an example of which is shown in Fig. 7(a). Note that this condition is limited to high-speed operation, and thus, the "0 V" compensation has little effect and torque estimation is equivalent with and without this compensation.

It is important to observe that, for all cases, once the torque is known, it is possible to achieve even the speed from a power balance similar to (11).

Hence, the difference between the value measured at the motor shaft with a torque transducer and the online estimated torque value is given just by the windage and friction-loss effect.

V. Conclusion

Online average torque estimation in PM motors may be achieved through the phase-voltage sampling and the phase-current measurement. Accurate torque values are obtained without any rotational component and regardless of the current waveform.

Experimental results on a three-phase PM ac motor have successfully validated the performance of the online torque estimator in terms of the average torque estimation by comparisons with standard torque-transducer results. The theoretical correctness of the torque estimator is validated by its ability to accurately match the results from the $i-\psi$ energy-loop method. Given the generic nature of the torque estimator, the implementation of this scheme is possible for a wider range of electrical machine: brushless PM motors, induction motors, or switched-reluctance motors. Further work is necessary to extend the use of this estimation in the actual machine control to develop optimized motor-control strategies.

Appendix

TABLE II
Estimation of the Loop Energy. Control Angle, Gamma = 0

Current [A]	Speed [rpm]	Loop energy [J] Test data	Loop energy [J] Voltage sampling (12)
0.65	400	1.70	1.70
	600	1.73	1.71
	800	1.62	1.62
	1000	1.57	1.53
1.00	400	2.70	2.70
	600	2.67	2.65
	800	2.63	2.55
	1000	2.48	2.44
1.35	400	3.65	3.70
	600	3.63	3.61
	800	3.48	3.42
	1000	3.38	3.30

Acknowledgment

The authors would like to thank P. Scavenius, N. C. Weihrauch, and P. E. Hansen of Danfoss Compressors, Flensburg, Germany, who supplied the special test motor used in this paper.

References

[1] T. J. E. Miller, M. Popescu, C. Cossar, and M. I. McGilp, "Computation of the voltage-driven flux–MMF diagram for saturated PM brushless motors," in *Conf. Rec. IEEE IAS Annu. Meeting*, 2005, vol. 2, pp. 1023–1028.

[2] D. A. Staton, R. P. Deodhar, W. L. Soong, and T. J. E. Miller, "Torque prediction using the flux–MMF diagram in AC, DC, and reluctance motors," *IEEE Trans. Ind. Appl.*, vol. 32, no. 1, pp. 180–188, Jan./Feb. 1996.

[3] F.-J. Lin, "Real time position controller design with torque feedforward control for PM synchronous motor," *IEEE Trans. Ind. Electron.*, vol. 44, no. 3, pp. 398–407, Jun. 1997.

[4] J. Solsona, M. I. Valla, and C. Muravchik, "Non linear control of a permanent magnet synchronous motor with disturbance torque estimation," *IEEE Trans. Energy Convers.*, vol. 15, no. 2, pp. 163–168, Jun. 2000.

[5] M. A. Rahman and M. A. Hoque, "On-line adaptive artificial neural network based vector control of permanent magnet synchronous motors," *IEEE Trans. Energy Convers.*, vol. 13, no. 4, pp. 311–318, Dec. 1998.

[6] R. Wu and G. R. Slemon, "A permanent magnet motor drive without shaft sensors," *IEEE Trans. Ind. Appl.*, vol. 27, no. 5, pp. 1005–1011, Sep./Oct. 1991.

[7] T. J. E. Miller, M. I. McGilp, and M. Olaru, *PC-FEA 5.5 for Windows—Software*. Glasgow, U.K.: SPEED Lab., Univ. Glasgow, 2006.

[8] O. Montero Hernandez and S. A. Bautista Cadena, "Design of a flux and torque estimator for a three-phase induction motor," in *Proc. CIEP*, Oct. 16–19, 1995, pp. 39–42.

[9] C. Lascu and A. M. Trzynadlowski, "A TMC320 C243-based torque estimator for induction motor drives," in *Proc. IEEE-IEMDC*, 2001, pp. 733–735.

[10] G. Buja, R. Menis, and M. I. Valla, "Disturbance torque estimation in a sensorless DC drive," *IEEE Trans. Ind. Electron.*, vol. 42, no. 4, pp. 351–357, Aug. 1995.

[11] R. Sepe and J. Lang, "Real-time observer-based (adaptive) control of a permanent-magnet synchronous motor without mechanical sensors," *IEEE Trans. Ind. Appl.*, vol. 28, no. 6, pp. 1345–1352, Nov./Dec. 1992.

[12] M. Bodson, J. Chiasson, R. Novotnak, and R. Rekowski, "High-performance nonlinear feedback control of a permanent magnet stepper motor," *IEEE Trans. Control Syst. Technol.*, vol. 1, no. 1, pp. 5–13, Mar. 1993.

[13] N. Ertugrul and P. Acarnley, "A new algorithm for sensorless operation of permanent magnet motors," *IEEE Trans. Ind. Appl.*, vol. 30, no. 1, pp. 126–133, Jan./Feb. 1994.

Calum Cossar was born in Hamilton, U.K., in 1962. He received the B.Sc. degree (with honors) in electronics and electrical engineering from the University of Glasgow, Glasgow, U.K., in 1983.

From 1983 to 1988, he was with Ferranti plc, Edinburgh, U.K., where he worked on the design of high-speed digital-signal processing for airborne-radar applications. In 1988, he joined as a Research Assistant the SPEED Laboratory, Department of Electronics and Electrical Engineering, University of Glasgow, where he is currently a Research Technologist and has been involved in research and development into the implementation of switched-reluctance control.

Mircea Popescu (M'98–SM'04) was born in Bucharest, Romania. He received the M.Eng. and Ph.D. degrees in electrical engineering from the University "Politehnica" of Bucharest, Bucharest, in 1984 and 1999, respectively, and the D.Sc. degree in electrical engineering from Helsinki University of Technology, Espoo, Finland, in 2004.

He has over 20 years experience in industrial research and development as a Project Manager with the Research Institute for Electrical Machines, Bucharest, and as a Research Scientist with the Electromechanics Laboratory, Helsinki University of Technology. Since 2000, he has been with the SPEED Laboratory, Department of Electrical and Electronics Engineering, University of Glasgow, Glasgow, U.K., where he has been a Research Associate Fellow. His main research interest includes modeling and optimization of the ac machines and drives.

T. J. E. Miller (M'74–SM'82–F'96) was born in Wigan, U.K. He received the B.Sc. degree from the University of Glasgow, Glasgow, U.K., and the Ph.D. degree from the University of Leeds, Leeds, U.K.

From 1979 to 1986, he was an Electrical Engineer and Program Manager with GE Research and Development, Schenectady, NY. His industrial experience includes periods with GEC (U.K.), British Gas, International Research and Development, and a student apprenticeship with Tube Investments Ltd. He is currently a Professor of electrical power engineering and Founder and Director of the SPEED Consortium with the SPEED Laboratory, Department of Electronics and Electrical Engineering, University of Glasgow. He is the author of over 100 publications in the fields of motors, drives, power systems, and power electronics, including seven books.

Prof. Miller is a Fellow of the Institution of Electrical Engineers, U.K.

Malcolm McGilp was born in Helensburgh, U.K., in 1965. He received the B.Eng. degree (with honors) in electronic systems and microcomputer engineering from the University of Glasgow, Glasgow, U.K., in 1987.

From 1987 to 1996, he was a Research Assistant with the SPEED Laboratory, Department of Electronics and Electrical Engineering, University of Glasgow, where he has been a Research Associate since 1996. He is responsible for the software architecture of the SPEED motor-design software and has developed the interface and user facilities, which allow it to be easy to learn and integrate with other PC-based software.

Mircea Olaru received the M.Sc. degree in mathematics from Bucharest University, Bucharest, Romania.

He has more than 35 years experience in finite-element analysis in electromagnetics and mechanics. He is currently an Analyst and Programmer with ICNDMF-CEFIN, Bucharest. He has authored 35 published articles and has presented 54 essays at national and international scientific meetings.